ARTICLE

# Soft XAS as an *in situ* technique for the study of heterogeneous catalysts

Received 00th January 20xx,
Accepted 00th January 20xx

DOI: 10.1039/x0xx00000x

Simon Beaunont,*[a]

Soft x-ray absorption *in situ* studies of heterogeneous catalysts have been applied to areas such as copper methanol oxidation catalysts and cobalt Fischer-Tropsch type catalysts over a period of around two decades. The technique has the potential to offer several advantages for studying heterogeneous catalysts against hard x-ray XAS in the systems that can be studied (includes elements such as C, N, O), the potential surface sensitivity (crucial for catalysts, where reactions occur at surfaces) and the information content of the resulting spectra. Nevertheless, it is technically challenging and the necessary hardware has only been developed and evolved in a few specific groups worldwide. This perspective will introduce the technique in the context of other competing spectroscopies, summarise the development of hardware and the challenges that have been overcome in experimental terms, along with the outcome and impact on different fields within catalysis. Additionally, anticipated future trends and directions will be discussed.

## 1 Introduction

In recent decades, catalysis research has developed a major focus on *in situ* or *operando studies*,[1-3] after identification of a significant "pressure-gap" between real catalytic process and many of the characterisation techniques deployed to interrogate catalyst materials.[4] A good illustration of this phenomenon is the restructuring of stepped Pt(557) single crystals on exposure to CO gas, small clusters of Pt are pulled out of the surface in trimer islands as the pressure increases from vacuum to ~1.3 mbar CO, but then returns to a stepped structure when re-evacuated.[5] Real catalytic reactions are known to exhibit mechanistic changes resulting from changes in pressure regime, an obvious example being the conversion and selectivity changes during benzonitrile hydrogenation that result from palladium hydride formation in Pd/$\gamma$-$Al_2O_3$ catalysts above a certain threshold pressure (~10 bar).[6] Such examples serve to illustrate the necessity of studying catalyst materials under conditions pertinent to their real world operation.

In the context of in-situ techniques, x-ray-based spectroscopy is ubiquitous, in major part due to the ability of x-rays to penetrate into catalytic reactor setups. X-ray absorption spectroscopies (XAS, Near-Edge x-ray absorption fine structure (NEXAFS, or sometimes XANES) and EXAFS (Extended Edge x-ray absorption fine structure) are frequently employed to study catalysed processes under reaction conditions using synchrotron radiation. These techniques are additionally very element specific: incident photons are absorbed to give electron energy transitions, which have different energies for different elements. A typical spectrum is shown in Figure 1a. The NEXAFS region of the spectrum covers excitation near to the threshold for electron ionisation (or 'edge') and includes excitations to unfilled orbitals (antibonding orbitals, Rydberg states or unfilled parts of a density of states plot in a solid).[7] The NEXAFS region (around the absorption edge) can therefore give information about chemical environment, such as formal oxidation state, symmetry or local charge distribution. Complementary to this, the EXAFS region of the spectrum results from photo-electrons that are completely ejected from the atom, but may be subjected to backscattering by electron clouds around their near neighbours (resulting in oscillation as a function of x-ray energy). These provide information about the local environment, specifically the number and type of coordinating atoms and the distances to these neighbours.[8] The measurement of the overall spectrum of this type is typically carried out by monitoring a sample's transmission of the relevant electromagnetic wave versus the intensity incident on the sample (a Beer-Lambert type absorption experiment). Alternatively, for both dilute samples and those where surface sensitive information is sought, indirect methods may sometimes be advantageous. In particular, x-ray fluorescence, Auger electron emission and total electron yield (TEY) measurements can all be utilized to indirectly monitor x-ray absorption, Figure 1b. In the presence of gases and of relevance to the discussion below, a few studies have also employed "conversion electron yield" (CEY) in which the TEY signal is modified by charge multiplication in the gas phase and collected by a bias voltage applied between sample and nearby electrode plate.[9, 10]

In general, such *in situ* measurements have been dominated by studies of catalyst structure using hard x-rays (> 5 keV) – this includes K-edge studies of 1$^{st}$/2$^{nd}$ row transition metals and L-

[a] Department of Chemistry, Durham University, South Road, Durham, DH1 3LE, UK. simon.beaumont@durham.ac.uk

Electronic Supplementary Information (ESI) available: [details of any supplementary information available should be included here]. See DOI: 10.1039/x0xx00000x

edges of third row transition metals and f-block elements. In vacuum systems, however soft x-rays (< 1 keV) have been widely used to study the absorption and orientation of molecules on surfaces (especially single crystals),[7, 11-13] but also nanoparticles[14, 15] as well as the nature of carbonaceous deposits on catalysts[16] or antiwear films.[17] Intermediate or tender x-rays in the 2-4 keV region have been used to study the fate of surface chloride and its influence on the preparation of catalysts derived from chlorine containing precursors in a flow cell with polycarbonate windows.[18] For elements such as Cl, S and P (2-3 keV), or the elements such as C, N and O (280 – 550 eV) commonly found in organic materials, the highest energy (1s electron ionisation) K-edges are already low energy enough to only be found in this tender or soft region of the x-ray spectrum. For other transition metals, soft x-rays also allow the L-edge XANES (*e.g.* 2p-3d transitions) rather than the K-edge to be studied, which are especially sensitive to oxidation state, structural symmetry and spin information.[19, 20]

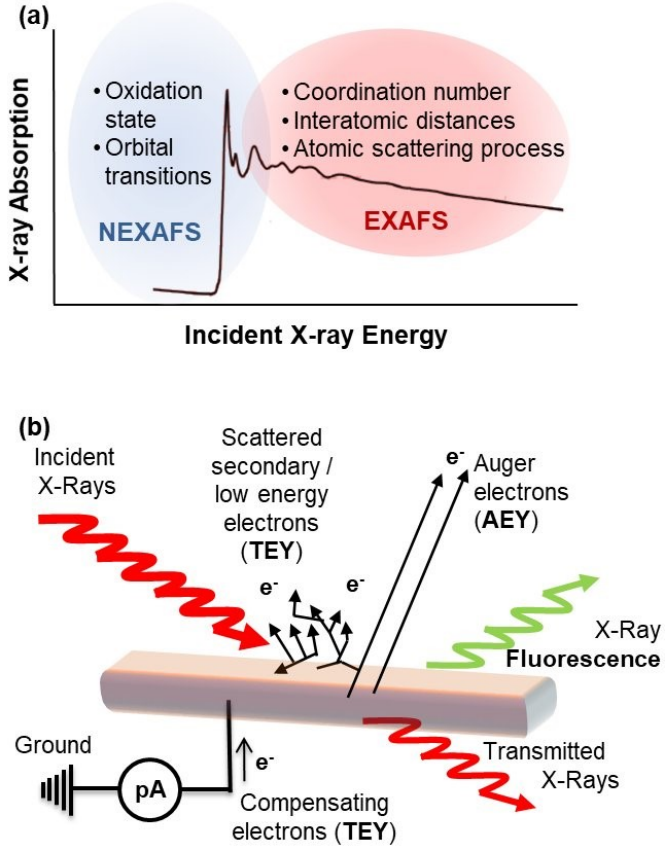


**Figure 1.** Schematics of (a) a typical x-ray absorption spectrum, including information contained in each region and (b) processes occurring during X-ray absorption by a sample, including measurement of the TEY current by placing a sensitive ammeter between the sample and ground.

Near-ambient pressure x-ray photoelectron spectroscopy (NAP-XPS), while not XAS, is worth briefly mentioning since it has also been used for *in situ* type studies including low x-ray energy elements and provides detailed oxidation state information.[21, 22] This technique is generally limited in gas pressure by the escape of the photo-electron: practically, this means significantly less than 1 atmosphere (0.1–15 mbar - although importantly, compared to high vacuum, these conditions imply the rate of molecules impinging on the surface is much greater than the TOF and so not rate limiting).[23] Since photoemission can in theory be conducted with higher energy photons and higher kinetic energy photoelectrons (it is the difference being measured) this limit is being pushed upwards by the use of "tender-NAP-XPS", where the incident photon is > 1 keV, but such methods are still in their infancy.[24] Another development in the field of ambient pressure XPS of potential interest to soft X-ray XAS practitioners too has been the use of ultra-thin graphene-based windows, through which a photoelectron can easily pass, but differences of up to 1 bar across the membrane have allowed *in situ* measurement of gold or copper nanoparticles.[25-27] The demonstration that such graphene-based windows can hold a difference of > 1 bar could be attractive in the soft X-ray range, where conventional XAS windows are still significantly attenuating.

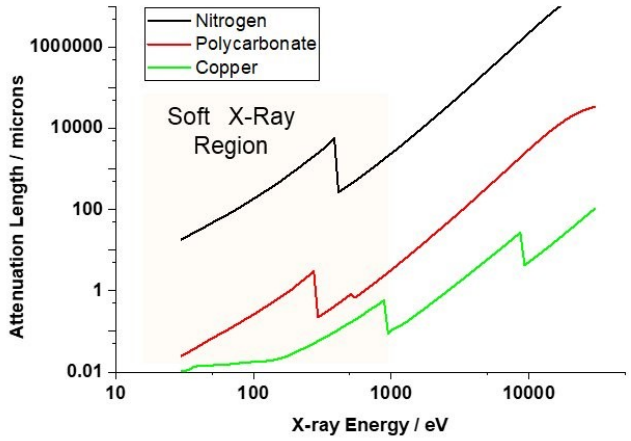


**Figure 2.** Attenuation lengths (distance to fall to $1/e^{th}$) as a function of x-ray energy for transmission through different materials (nitrogen gas, polycarbonate plastic or solid copper). Data obtained from Henke *et al.*.[28]

In situ XAS at x-ray edges that fall in the soft region is attractive for the reasons set out above (accessing light elements and greater information content of L-edges), but by contrast faces the challenge that the attenuation lengths of soft x-rays are substantially less than that of their harder counterparts (Figure 2). One route to overcome this is simply to dramatically reduce the transmission path. This has been attempted for the study of Cyanopyrazine hydration on $TiO_2$, where a cell with 100 nm thick windows (of SiC or $Si_3N_4$) and a path length of as low as 20 nm were used to obtain transmission spectra.[29] This approach has been extended to electrochemical systems.[30] While demonstrated possible, the small cell volume may not be suited to many typical catalyst studies. Another route is to use a setup similar to that employed for NAP-XPS, where Auger electron yield can be measured by tuning the spectrometer to collect the emitted Auger electrons.[22, 31-34] This approach, however, suffers the same drawbacks in achievable pressure as NAP-XPS. A more generalizable approach that makes use of total electron yield measurement has been gradually developed over the past ~20 years (predominantly in Berlin, Germany and Berkeley, USA). In

this approach, the incident x-ray results in electron emission (predominantly Auger and secondary electrons) from the sample, producing a small current from the sample to ground that can be measured using the current pre-amplifiers (*e.g.* Keithley picoammeters) commonly used for ionisation chambers at XAFS beamlines (Figure 1b). Since the electrons emitted are not being measured, the technique's penetration into the sample environment depends only on the incident x-ray. This allows a small environmental cell with an x-ray transparent window to maintain control of the sample conditions. This article gives an overview of the development of such soft x-ray XAS experiments and the insights into catalytic chemistry provided by such studies, along with a perspective on current limitations and future directions of this approach.

## Design, Evolution and limitation of *in situ* cells for soft XAS I: Berlin

The initial development of a cell by Knop-Gericke and coworkers was reported in 1998.[35, 36] Their aim was to develop a cell for TEY yield measurement. Transmission was identified to be unsuitable because single crystals and thin film substrates are generally too thick to be penetrated by low energy x-ray beams. Soft x-rays were necessitated by a desire to look at the conversion reactions of organic molecules and therefore the low Z elements carbon, nitrogen and oxygen. Fluorescence mode, while possible, can generate experimental artefacts such as thickness effects and self-absorption. TEY mode is also advantageous due to its greater surface sensitivity (a few nm – although the exact mechanism has been a point of controversy[37-39]). On the basis the first "tank reactor" cell was produced in which 4 signals ($I_0$ – $I_3$) were recorded (shown schematically in Figure 3), and the x-rays enter the cell *via* a polyimide window. By normalising $I_2$ (which collects gas phase signal and some sample signal) by division with $I_1$ (the gas phase signal alone – based on calculated distance and bias conditions needed for collection of low energy electrons[40] and comparison with high resolution O K-edge data for molecular oxygen), they demonstrated that the sample signal could be extracted without a dominant contribution from gas phase electron quenching. By collection of the electrons emitted through the gas to the TEY collection plate ($I_2$), it is not clear to what extent similar amplification processes occur as those reported previously as "conversion electron yield",[9, 38] although the lower energy of the electrons being emitted will partially reduce the extent to which this can occur (*e.g.* the ionisation threshold requires a minimum of 24.6 eV (He), 12.1 eV ($O_2$), or 10.8 eV (methanol)[41] per extra electron generated by the amplification process). Such gas phase quenching is a major problem for most gases except $H_2$ and He. Despite showing it was possible to overcome significant gas phase quenching in this way, the overall path of x-rays through the gas chamber was 25-43 mm, and the authors noted this long x-ray gas path restricted the total pressure. The temperature of the sample was controlled by the use of an inert ceramic heater. The key details of this and all the "tank reactor" type cells described are given in Table 1.

The gas phase contribution ($I_1/I_0$) was shown in a subsequent paper to allow collection of gas phase reaction data from the sample environment.[42] Further modification of the procedure for normalisation was adopted to extract O K-edge data from the dominant gas phase signal.[42] This involved obtaining the sample spectrum as a difference spectrum resulting from the subtraction of $I_1/I_0$ (gas only) from $I_2/I_0$ (gas and sample), such that no negative intensity is seen in the sample signal. It should be noted this is effectively the same as normalisation by the size of the molecular oxygen $\pi^*$ component from the gas phase described in a subsequent paper,[43] as the gas phase oxygen $\pi^*$ component at 530.8 eV is a distinctive feature below the energies of the surface signals. In subsequent papers a similar method was employed for observation of the nitrogen K-edge through ammonia gas, but normalisation instead uses the sharp N-H $\sigma^*$ resonance from the gas phase ammonia to obtain the surface only contribution.[44, 45] It was also noted that observation of the copper L-edge was not significantly effected by the gas phase and the surface copper spectrum could be retrieved from either the sample($I_2/I_0$) or the collection plate($I_3/I_0$).[44] The same setups have been used to record Fe L-edge spectra of Fe/ZSM-5 and the benefited from the much higher resolution of soft x-rays compared with hard x-rays along with the relatively large, systematic variation of the spectral features in the metal (Fe) L-edge with the oxidation state. This combined with the surface sensitivity of the technique (here cited as 4 nm[46]) provides a useful *in situ* technique for studying such materials as catalysts.

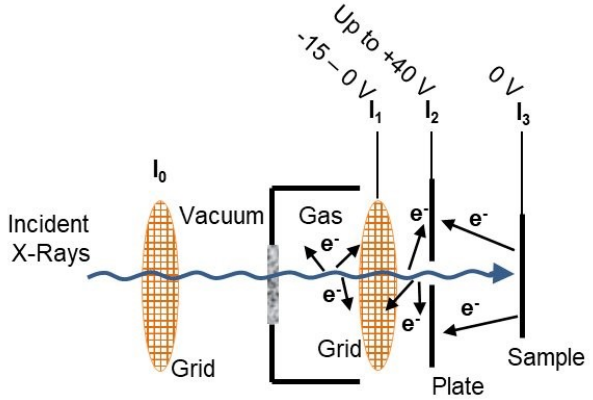


**Figure 3.** Schematics of reactor "tank" cells described in papers by Knop-Gericke *et al.*,[35] showing basic setup of in situ gas cell. The four currents $I_0$-$I_3$ are measured using a current preamplifier (e.g. Keithley), between the contact point and ground. Ranges of bias voltages used in experiments are indicated.

While not strictly soft x-ray, it is useful to note a complementary setup was developed in Utrecht and used for 1000 – 3500 eV x-rays, which are still significantly attenuated by the gas phase.[47, 48] This was used for measurement of the Al K-edge spectra in zeolite beta under a flow of He gas at Daresbury, UK. The cell design specifically incorporates a gas proportional counter near the sample (benefiting from solid angle) to obtain fluorescence signal – in this context it is noted a thicker larger diameter fluorescence collection window (and corresponding greater solid collection angle) is more desirable than a thinner smaller diameter version. Care was taken in the design to use amplifiers

close to the detector for both TEY or fluorescence detectors and avoid unnecessary magnetic or electrical heaters (the furnace used a counter wound heating element, powered by a stabilised d.c. power supply). A collector plate is included in the design for TEY signal collection (or CEY collection if the plate is biased to take advantage of gas phase amplification).

## Design, Evolution and limitation of *in situ* cells for soft XAS II: Berkeley

Initial experiments with Cu L-edge XANES were conducted by the Bell group using a scanning x-ray transmission microscope (STXM) beamline and employing an etched "lab on a chip" reactor in transmission mode with particles picked up manually on a $Si_3N_4$ membrane window.[49] This approach enabled a gas path of only 0.8 mm, overcoming the limitations of pressure limits previously described and operating instead at 1 bar in gases such as 4% CO or 10% $O_2$ (He balance), and achieving heating by an Al resistive heater assembled directly on the chip. This approach enabled spectral acquisition for the first time at more catalytically relevant pressures, but the need to use minute (few ng) sample quantities, combined with the need to locate particles of uniform thickness makes it difficult to scale for comparisons to conventional flow reactors / flow patterns. Furthermore, the transmission mode detection scheme is a bulk analysis, in contrast to the possible surface sensitivity obtained from TEY measurements. Nevertheless, spectromicroscopy can be very beneficial for understanding the outcome of averaging techniques by allowing for interrogation of individual constituents of macroscopic samples.

X-ray emission spectroscopy studies were conducted at a similar time using a sealed polyimide X-ray window cell to probe the formation of sulfate at a water-solar cell absorber interface.[50] Subsequent to this chloride induced corrosion or iron surface in humidified air was followed using either diamond-like or $Si_3N_4$ windows and employing soft x-ray in / x-ray out techniques (fluorescence XAS along with x-ray emission spectroscopy and resonant inelastic x-ray scattering (RIXS)).[51] A similar RIXS-based approach was used to measure cobalt nanocrystals in solution encapsulated under a $Si_3N_4$ window – mentioned here as this is a clear forerunner to the *in situ* catalysis cells that follow from the same group.[52] In 2009, the first "tank reactor" appeared based on a sample placed in thermal contact with a button heater and mounted in a chamber of controlled gas environment close to a $Si_3N_4$ membrane window, to minimise the gas path.[52] A shielded cable spot-welded to the sample was used to obtain a TEY signal by connection to ground *via* a picoammeter. A schematic provided by the original authors is reproduced in Figure 4a. In this mode spectra at the Co L-edge were recorded in a variety of gas mixtures ($H_2$, CO or combinations thereof), while O K-edge spectra were obtained by first flushing oxygen containing CO out of the cell with He or $H_2$. A similar cell (Figure 4b) was found to be suitable for electrochemical cycling of a Cu film electrode in $NaHCO_3$ solution for study of electrolyte – the presence of the liquid limiting detection to x-ray in / x-ray out (fluorescence mode) only.[53] Such x-ray in/ x-ray out approaches have continued to be used with $Si_3N_4$ or SiC windows to monitor liquid-solid interfaces in the studies of various electrocatalytic systems.[54-56]

ARTICLE

**Table 1.** Summary of key details of all in situ reactor cells described in main text.

| Reference | Edge(s) measured | Max temperature / °C | Max pressure / bar | Window type | Beamline / Synchrotron |
|---|---|---|---|---|---|
| [35, 42, 57] | Oxygen K<br>Copper L | 727 | 0.02 | Polyimide (250 nm) coated both sides with AlN (30 nm) | HE-TGM1, BESSY |
| [43] | Oxygen K<br>Copper L | 497 | 0.01 | 200 nm polyimide | PM1 and HE-TGM1, BESSY |
| [44] | Nitrogen K<br>Copper L | 397 | 0.0012 (although can withstand 0.1) | 300 nm polyimide | U49/1-SGM BESSY II |
| [45] | Nitrogen K<br>Copper L | 397 | 0.0012 (although can withstand 0.1) | 100 nm $Si_3N_4$ | UE56/2-PGM1 BESSY II |
| [58, 59] | Iron L<br>Oxygen K | 350 | 0.01 | Presumed polyimide | U49/2-PGM-1 and UE56/2-PGM-1, BESSY II |
| [47, 48] | Aluminium K | 477 | 1 (up to 5 pre-treatment) | 7 μm in, 13 μm out Be | beamline 3.4, SRS Daresbury |
| [60] | Vanadium L | 400 | 0.002 | Presumed polyimide | U/49-2, BESSY II |
| [61] | Manganese L<br>Cobalt L | 425 | 0.002 | (method not certain) | U56/2<br>PGM-2 at BESSY II |
| [49] | Copper L | 260 | 1 | 100 nm $Si_3N_4$ | 11.0.2, ALS |
| [52] | Cobalt L<br>Oxygen K | 330 | 1 | 100 nm $Si_3N_4$ | 7.0.1. ALS |
| [62] | Cobalt L<br>Carbon K (data not shown) | 250 | 0.048 $O_2$, 1 total (He balance) | 100 nm $Si_3N_4$ | 7.0.1. ALS |
| [63] | Cobalt L | 230 | 0.347 ($CO_2/H_2$), 1 total (He balance) | 100 nm $Si_3N_4$ | 7.0.1. ALS |
| [64, 65] | Cobalt L | 225 | 1 ($H_2$) | 100 nm $Si_3N_4$ | 7.0.1. ALS |
| [66] | Cobalt L | 125 | 0.080 ($CO/O_2$), 1 total (He balance) | 100 nm $Si_3N_4$ | 7.0.1. ALS |
| [67] | Cobalt L | 260 | 2.7 ($CO_2/H_2$, 1:3) | 100 nm $Si_3N_4$ | 7.0.1. ALS |
| | Copper L | 175 | 4 ($H_2$) | | |
| [68] | Cerium M | 200 | 0.020 ($O_2$ or $H_2$) | 100 nm $Si_3N_4$ | 7.0.1. ALS |
| [69] | Cobalt L<br>Manganese L<br>Cerium M | 250 | 0.072 ($CO/O_2$) | 100 nm $Si_3N_4$ | 7.0.1. ALS |
| [70] | Cobalt L | 500 (250 shown) | 1 ($O_2$ or $H_2$) | 100 nm $Si_3N_4$ | 7.0.1. ALS |
| [71, 72] | Cobalt L<br>Oxygen K (He only) | 250 | 1 ($H_2$, $O_2$ or He) | 100 nm $Si_3N_4$ | 7.0.1. and 6.3.1 ALS |

A similar cell setup was developed in the Somorjai group, again consisting in a sample close to a $Si_3N_4$ membrane window, to minimise the gas path and with the signal measured by TEY signal (Figure 4c).[62] The heating mechanism, thermocouple and shielded signal cable were passed out of the cell along a long metal tube to allow the reactor "tank" to be located in the beam from a gate-valved port and linear drive assembly some distance off the beam axis of the UHV chamber in which the setup was mounted. The $Si_3N_4$ window contained within the cap (black in Figure 4c) was attached over two spring loaded Viton fluoroelastomer O-rings (white in diagram) that allowed electrical isolation and separate grounding of the cap *via* a wire screwed to the cap, while also providing a seal sufficient to separate > 1 bar gas from UHV with a minimal leak rate. The sample was again heated by use of a BN button heater underneath the sample, which comprised of nanoparticle catalysts deposited on a gold foil to be studied. The seals (rated to 205 °C) proved an Achilles' heel of this design when pushing the cell to higher temperatures, upon which (even though the seals are not adjacent to the heat source) a leak would often

result in aborting heating of the sample. This method was employed combined with a least squares fitting approach of the step-edge normalised cobalt L-edge spectra obtained to a series of reference compounds. Carbon K-edge data were collected (although not shown) in the presence of the $He/O_2$ mixture at a total pressure of 1 bar. Due to concern about the interaction of metal nanoparticles with the gold foil substrate on heating, in subsequent work on $CO_2$ hydrogenation over CoPt nanoparticles, the native oxide layer of a silicon wafer surface was instead used for Langmuir Blodgett deposition of nanoparticles, being sufficiently conducting for collection of the TEY signal in the same way.[63] The cell was ultimately operated as high as 4 bar pressure in pure $H_2$, or 2.7 bar in a reactive mixture of $CO_2$ and $H_2$.[67] It is noteworthy that, although unsuccessful (probably due to the problems of even nanoparticle deposition), attempts were made around this time to deposit the sample on the window. This would mean the soft x-rays need not penetrate the gas to get to the sample and a bias voltage could be applied to the original sample holder to attempt removal or minimisation of the gas phase signal (*e.g.* when recording O or C K-edge spectra in $CO_2$).

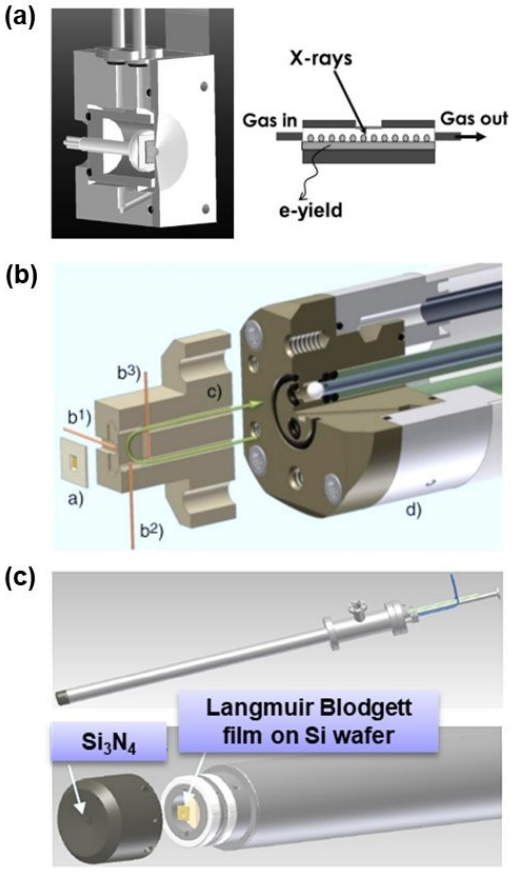


**Figure 4.** Schematics of reactor cells. (a) Herranz *et al.*,[52] showing basic setup of in situ gas cell. (b) Jiang *et al.*,[53] showing electrochemical cell assembly comprising, a, $Si_3N_4$ window, b1, electrical connection to $Si_3N_4$ window (working electrode), b2, reference electrode, b3, counter electrode, c, PEEK body, d, support tube assembly. The green arrow indicates the liquid flow. (c) Zheng *et al.*,[62] showing assembly of gas cell and sealing system used for *in situ* studies. (reproduced with permission from references given).

The next significant reported change to cell design was reported by Escudero *et al.*, and the primary innovation over the cells described above was the change of sample heating method to use an 18A, 10 W, 975 nm CW laser coupled to the sample *via* a fibre optic.[70] In particular, this prevents signal transmission problems caused by the presence of high current heating wires near the signal transmission cable. Furthermore, it prevents the presence of resistive heating elements that may become exposed to reactive gases, *via* micro-fracturing of the ceramic, and modify the species observed on the catalyst. An additional improvement was made to this generation to include gold coating of the internal metal work and avoid alloys being contacted with the gas that might generate metal carbonyls. The window was affixed in the cap with a non-conducting epoxy, but the cap could be independently biased to minimise the effect of electrons from gas phase molecules on the sample signal or on the window. The subsequent studies of O K-edge spectra during CO hydrogenation necessitate sweeping out the cell with He to remove oxygen-containing species, even with the mentioned cap-biasing capability.[71, 72] A similar silicon nitride window assembly has recently be demonstrated for use in *in situ* studies of copper and cerium oxide powders at the APE-HE beamline at the Elettra lightsource in Trieste, Italy.[73]

## New insights in heterogonous catalysis from soft XAS

The work enabled by the cell development and use of soft x-ray spectroscopy at approaching realistic pressures has made a marked and lasting impact on a number of fields within heterogeneous catalysis. Complementary to the discussion of how such measurements can be achieved and the necessary hardware development, it is instructive to look at some of the examples of systems where significant new insights have resulted.

In the case of methanol oxidation, studies by Knop-Gericke and co-workers were able to show for copper catalysed methanol oxidation that a weakly bound oxygen species was present only when methanol and oxygen were also present. A structure activity correlation between this oxygen species and formaldehyde production was established.[42] This species was assigned as suboxide including O2p-Cu4sp hybridisation (in contrast to oxygen hybridising with Cu3d found in other copper oxide structures).[43] Such species had been discussed theoretically and identified under UHV conditions for silver epoxidation catalysts,[36] but the use of soft x-rays allowed observation of a spectroscopic signature of a species that correlated with the production of the desired formaldehyde product.

Some time later, in 2013, Knop-Gericke and co-workers also investigated the use of a Berkeley type cell design to study both thin film (coated on window) and powdered silver epoxidation catalysts using a mixture of TEY, Fluorescence Yield and RIXS to identify specific atomic oxygen species.[74] A gap of only tens of μm was used between the powder and the window to reduce the gas signal to a minimum, although further investigation is

 

required to establish if this may cause mass transfer limitations as discussed in the paper and normalisation to remove molecular oxygen signals still had to be employed.

Studies of ammonia oxidation, a reaction important in the treatment / clean-up of exhaust gases or the purification of feed-streams of hydrogen for fuel cell applications, again benefited from soft x-ray XAS to establish structure activity relationships.[44] Firstly, it could be seen that small increases in pressure (1.2 vs. 0.4 mbar) could prevent copper nitride formation, which poisoned the reaction on short timescales. Secondly, in this reaction it is highly important to avoid over-oxidation to NO rather than $N_2$, due to the toxicity of the former. The authors showed the desired reaction to $N_2$ could be correlated with $Cu_2O$, while unwanted NO production resulted from the presence of CuO. As before polycrystalline copper foil had been used as a catalyst mimic, but a subsequent study shows that the same general structure-activity correlations (although at slightly lower temperature) could be seen for Cu particles (~ 2.8 nm), which were prepared on a carbon coated gold TEM grid using a gas aggregation technique.[45] It is of course fortuitous (or a good reaction choice) that the pressure range accessible with the soft XAS setup used (< few mbar) and the pressure range in which marked changes in reactivity were established (0.4 vs 1.2 mbar) were well aligned. For this series of papers, a clear question must be asked as to the effect of increasing the pressure again by a factor of ~$10^3$ to pressures of real world catalytic relevance.

Soft x-ray XAS has also found application in the study of redox chemistry in the iron containing zeolite ZSM-5, which is used and/or has potential as a catalyst for a number of processes.[58, 59] The study takes advantage of the information rich metal L-edge spectra with complementary theoretical calculations to understand the lineshape obtained using charge-transfer multiplet calculations. These are well-described elsewhere,[19] and especially suited to partially filled 3d metals,[75] but essentially consist in accounting for charge transfer from surrounding orbitals (*e.g.* O 2p in iron oxides) into the metal 3d to improve the agreement with experimental spectra. Using this more theoretical approach to spectral interpretation it was possible to show that although the iron present in this catalyst is still in an octahedral co-ordination sphere, the crystal field splitting is much weaker than in bulk $Fe_2O_3$, indicating weak Fe-O bonding that may help rationalise its substantially different catalytic behaviour.

Vandium phosphorous oxide catalysts are used to produce maleic anhydride by oxidation of n-butane, an important intermediate in the production of polyester resins. While the main crystalline phase is known to be vanadyl pyrophosphate $(VO)_2P_2O_7$, the nature of active sites was poorly understood. Soft x-ray spectroscopy was used to show it is likely that there is a dynamical interaction of different phases on the active surface of vanadyl phosphate.[60] In particular, a number of resonances could be fitted in the V-L edge spectra that changed in ratio (and therefore abundance) at different temperatures, with certain resonances correlating with activity. This shows that a number of vanadium containing species were present on the working catalyst, only some of which were active, and the number of active sites varied with temperature. As an aside, this causes a significant problem for interpreting apparent activation energy in these systems as the assumption of a fixed number of active sites and changing temperature is not valid.

Morales *et al.* extended the use of soft x-ray TEY XAS to cobalt and cobalt manganese Fischer Tropsch catalysts supported on TiO2.[61] Here, the key advantage of XAS over other measurements is that it is element specific and so (in contrast to *e.g.* temperature programmed reduction) it is able to monitor the oxidation state of one element (cobalt) to high degree of accuracy. L-edge spectra often show more structure dependence on redox state, hence the use of L-edge over hard x-ray K-edges could be justifiable in this case, where the goal of studying the three metals (Ti, Co and Mn) is to elucidate oxidation states. The key finding in this case was that both Mn as an additive and $TiO_2$ as a support render the cobalt component harder to reduce, with more higher oxidation state cobalt present. This correlated with supressed absolute activity, but increased $C_5$+ yield – suggesting dual roles for Co and CoO in the reaction.

Cobalt containing Fischer-Tropsch type catalysts have been studied further using soft x-ray TEY XAS in the groups of Salmeron and Somorjai in Berkeley. The cobalt L-edge is especially sensitive to oxidation state and least squares fitting to reference compounds can readily be used to estimate the extent of oxidation. [62, 76] In order to try and understand particle size effects—it has been demonstrated for the Fisher-Tropsch reaction that particles of at least a threshold size (4-6 nm) are required)[77, 78]—size controlled nanoparticles were prepared by decomposition of $Co_2(CO)_8$ in the presence of templating agents, trioctylphosphine oxide (TOPO) and oleylamine. Soft x-ray TEY XAS showed that when these nanoparticles (as prepared) were deposited on a gold foil and heated in hydrogen to 330 °C, the large particles were slower to reduce. Experiments exposing the resulting reduced cobalt to $CO/H_2$ and re-evacuating never resulted in re-oxidation, but some evidence for water was seen at the O K-edge. The conclusion that large cobalt particles are harder to reduce is rather unexpected (a priori, smaller particles contain more co-ordinatively unsaturated atoms that would favour oxidation). It is also the converse of the size-dependant oxidation-state behaviour exhibited by other metals such as rhodium,[79] or the ease of reducibility as a function of size found by others working on size controlled cobalt nanoparticles[80] (though it should be noted CoO has been suggested to be unimportant based on hard x-ray XAS in the reason for the lower activity of small Co particles[77, 81]). The reasons for this are unclear, though the same study reports reduction at 650 °C for the corresponding catalyst measurements (and $CH_4$ seen to be being removed from 550-650 °C suggesting significant surface contamination from residual synthesis agents (*e.g.* capping agents) at these temperatures). The use of TOPO was also subsequently found to be problematic in obtaining hydrogenation activity from similar nanoparticles,[64] or as noted above there is some doubt as to the stability of cobalt particles on gold foil (the substrate was subsequently replaced with Si wafers), as shown by the mobility present in gold-cobalt alloys at 250-300 °C during bulk

processing.[82] Equally, further studies would be required to establish whether the slowness of reduction for the larger particles was the consequence of being less thermodynamically favourable or just kinetic slower. Nevertheless, the demonstration of using soft x-ray XAS in the presence of 1 bar gas still represents a step change in the applicability of the data acquired to real catalytic systems.

Further studies using this type of approach have also demonstrated that CO dissociation occurs more readily over larger particles and hydrogen dissociation is seen to promote CO dissociation (the authors argue this points to a "hydrogen assisted" type mechanism).[71] The pressure dependence up to 4 bar in hydrogen of the cobalt oxidation state has been observed, showing that significant changes in the reduction temperature exist as a function of pressure for cobalt nanoparticles.[67] It has also been possible to show that precious metal promotors operate *via* a hydrogen spill-over mechanism by observing the effect of discrete Pt particles on nearby Co particles during reduction. This experiment takes advantage of the element specific nature of XAS and the sensitivity afforded by the pronounced difference in the line shape of the metal L-edges as a function of oxidation state.[65]

Alloyed CuCo containing catalysts have also been suggested as effective catalysts for Fischer-Tropsch, and the possible production of oxygenates.[83] Interrogation of nanoparticles synthesized to contain copper and cobalt with soft x-ray XAS is possible at both the copper and cobalt L-edges and has been used to show: (i) the Cu and Co segregate reversibly under oxidising or reducing gases, (ii) both remain reduced under $CO_2$ methanation conditions, and (iii) the copper facilitates lower temperature reduction of the cobalt.[67] An interesting dealloying behaviour of the two metals into Cu rich and Co rich phases also resulted in observation by XANES of partial oxidation of the Co rich phase in CO, pointing to a significant gap in our understanding of this system still to overcome.[72]

Other studies using soft x-ray XAS focussed more on catalyst materials have shown the impact of platinum on the ease of oxidation/reduction of cobalt under varying gas and pressure conditions,[62, 66] and the on $CeO_2$ as a result of hydrogen spillover causing $Ce^{3+}$ states to form (observed at the Ce M-edge).[68] The enhancement of CO oxidation rate over various oxides ($Co_3O_4$, $MnO_2$ and $CeO_2$), was also linked to the demonstrated redox properties of the supporting oxides using soft x-ray XAS.[69] Finally, changes in sintered $LaCoO_3$-based materials have been examined successfully at the oxygen K-edge using a small sample-window gap and dilute (up to 1%) oxygen containing gas streams.[84]

## Wider discussion and developments in soft XAS (theory and experiment).

TEY yield measurement of the kind described extensively above affords a unique advantage of relative surface sensitivity in so far as catalysis is concerned. This is always an important merit of any characterization tool in this field. Nevertheless, a number of developments in the corresponding x-ray emission or RIXS and selective x-ray absorption processes,[19] which can be performed using the fluorescence yield mode should not be entirely overlooked. RIXS in essence is the tuning of the excitation to a particular part of the absorption edge and monitoring the emission spectrum that results. Until recently this photon hungry technique has been limited by the need to have very high brilliance sources and the necessary advanced photon detection.[85] It is envisaged that this technique may be particularly useful in applications where charge transfer is important, whether used directly on a working catalyst system or an experimental tool to assign resonances within complex XANES lineshapes.

In the above discussion, it is clear the vast majority of catalytic *in situ* studies have conducted analysis by empirical interpretation and comparison to reference samples of known materials. With advances in the theory of core level spectroscopies that increasingly make calculations of spectra more feasible (in terms of computational expense), and newer approaches offering less dependence on a range of fitting parameters and more scope for *ab initio* calculations based on a material's structure,[75] calculations can be expected to be increasingly important in interpreting soft x-ray XAS. This is likely to enable better interpretation, particularly on the metal L-edges, as is partly exemplified using charge-transfer multiplet analysis in the case of Fe/ZSM-5 above.[19, 58]

One downside of ever more brilliant sources and techniques that depend on their high photon flux is the risk of sample damage – the reduction of samples by incident x-rays is more frequently considered for biological systems and diffraction experiments, but this merits consideration in studies of metals at their L-edges given a recent study showing reduction of Mn during L-edge XAS.[86]

## Conclusions and future perspectives

There are clear advantages for soft x-ray XAS as a probe for catalyst studies:

i. The relative surface sensitivity afforded by TEY measurements provides insight into the part of the material where catalysis actually occurs.
ii. The possibility of studying and quantifying light elements (C, N, O) that cannot easily be studied *in situ* by other means (they do not have hard x-ray accessible edges, other spectroscopies are less penetrating of sample environments, *e.g.* XPS, optical spectroscopies cannot always separate orientation of a functional group on a surface or the environment it is in to permit quantification of specific species). It has been possible to use soft x-ray XAS up to 4 bar (in hydrogen) to date.
iii. The oxidation state sensitivity and structural detail of the non-1s level transitions such as 3rd row transition metal L-edges is often greater than their K-edge counterparts.

Besides greater interaction with theory to calculate spectra and use of x-ray emission and RIXS to complement TEY measurements, the work described above shows the potential of further developments in the use of soft x-ray TEY cells to be

 

highly fruitful. A specific challenge may be in unifying the approach by groups at BESSY to measure both the gas phase and the gas + sample signal for use in processing the data and the approach in Berkeley of using short gas paths (the latter still prevented spectral acquisition in the presence of gases containing the element of interest). It is very likely that incorporating a better understanding of the x-ray gas interactions may allow more robust compensation schemes for removing the gas phase component of the signal, or else the improvements in component fabrication (e.g. additive manufacture) may allow the use of more complex/compact cell designs. In any case, the examples above show the opportunities offered by soft x-ray XAS studies to establish structure-activity relationships in catalysis – new understanding that is invaluable in the better design and operation of catalyst systems in real world applications.

## Conflicts of interest

There are no conflicts to declare.

## Notes and references


1. B. M. Weckhuysen, *Phys. Chem. Chem. Phys.*, 2003, **5**, vi-vi.
2. G. A. Somorjai, S. K. Beaumont and S. Alayoglu, *Angew. Chem., Int. Ed.*, 2011, **50**, 10116-10129.
3. J. A. Rodriguez, J. C. Hanson and P. J. Chupas, *In-situ Characterization of Heterogeneous Catalysts*, John Wiley & Sons, Inc., Hoboken, NJ, USA, 2013.
4. G. Rupprechter and C. Weilach, *J. Phys.: Condens. Matter*, 2008, **20**, 184019.
5. F. Tao, S. Dag, L.-W. Wang, Z. Liu, D. R. Butcher, H. Bluhm, M. Salmeron and G. A. Somorjai, *Science*, 2010, **327**, 850-853.
6. J. J. W. Bakker, A. G. v. d. Neut, M. T. Kreutzer, J. A. Moulijn and F. Kapteijn, *J. Catal.*, 2010, **274**, 176-191.
7. J. Stöhr, *NEXAFS Spectroscopy*, Springer, 1992.
8. B. K. Teo, *EXAFS: Basic Principles and Data Analysis*, Springer Berlin, Heidelberg, 1986.
9. G. D. Moggridge, T. Rayment, R. M. Ormerod, M. A. Morris and R. M. Lambert, *Nature*, 1992, **358**, 658-660.
10. G. D. Moggridge, S. L. M. Schroeder, R. M. Lambert and T. Rayment, *Nuclear Instruments and Methods in Physics Research Section B: Beam Interactions with Materials and Atoms*, 1995, **97**, 28-32.
11. B. Watts, L. Thomsen and P. C. Dastoor, *J. Electron Spectrosc. Relat. Phenom.*, 2006, **151**, 105-120.
12. F. Bournel, C. Laffon, P. Parent and G. Tourillon, *Surf. Sci.*, 1996, **350**, 60-78.
13. C. Sanchez-Sanchez, N. Orozco, J. P. Holgado, S. K. Beaumont, G. Kyriakou, D. J. Watson, A. R. Gonzalez-Elipe, L. Feria, J. F. Sanz and R. M. Lambert, *J. Am. Chem. Soc.*, 2015, **137**, 940-947.
14. C. M. Yim, C. L. Pang and G. Thornton, *Top. Catal.*, 2016, **59**, 708-724.
15. C. M. Yim, C. L. Pang, D. S. Humphrey, C. A. Muryn, K. Schulte, R. Pérez and G. Thornton, *Faraday Discuss.*, 2013, **162**, 191-200.
16. H. Shimada, M. Imamura, N. Matsubayashi, T. Saito, T. Tanaka, T. Hayakawa and S. Kure, *Top. Catal.*, 2000, **10**, 265-271.
17. Z. Yin, M. Kasrai, M. Fuller, G. M. Bancroft, K. Fyfe and K. H. Tan, *Wear*, 1997, **202**, 172-191.
18. P. B. J. Thompson, B. N. Nguyen, R. Nicholls, R. A. Bourne, J. B. Brazier, K. R. J. Lovelock, S. D. Brown, D. Wermeille, O. Bikondoa, C. A. Lucas, T. P. A. Hase and M. A. Newton, *J. Synchrotron Radiat.*, 2015, **22**, 1426-1439.
19. F. de Groot, *Chem. Rev. (Washington, DC, U. S.)*, 2001, **101**, 1779-1808.
20. X. Deng, X. Gu and F. F. Tao, in *Heterogeneous Catalysis at Nanoscale for Energy Applications*, eds. F. F. Tao, W. F. Schneider and P. V. Kamat, DOI: 10.1002/9781118843468.ch5, pp. 93-114.
21. H. Bluhm, M. Hävecker, A. Knop-Gericke, M. Kiskinova, R. Schlögl and M. Salmeron, *MRS Bulletin*, 2007, **32**, 1022-1030.
22. M. Salmeron and R. Schlögl, *Surf. Sci. Rep.*, 2008, **63**, 169-199.
23. S. K. Beaumont, S. Alayoglu, V. V. Pushkarev, Z. Liu, N. Kruse and G. A. Somorjai, *Faraday Discuss.*, 2013, **162**, 31-44.
24. S. Axnanda, E. J. Crumlin, B. Mao, S. Rani, R. Chang, P. G. Karlsson, M. O. M. Edwards, M. Lundqvist, R. Moberg, P. Ross, Z. Hussain and Z. Liu, *Scientific Reports*, 2015, **5**, 9788.
25. A. Kolmakov, D. A. Dikin, L. J. Cote, J. Huang, M. K. Abyaneh, M. Amati, L. Gregoratti, S. Günther and M. Kiskinova, *Nat. Nanotechnol.*, 2011, **6**, 651-657.
26. J. Kraus, R. Reichelt, S. Günther, L. Gregoratti, M. Amati, M. Kiskinova, A. Yulaev, I. Vlassiouk and A. Kolmakov, *Nanoscale*, 2014, **6**, 14394-14403.
27. R. S. Weatherup, B. Eren, Y. Hao, H. Bluhm and M. B. Salmeron, *The Journal of Physical Chemistry Letters*, 2016, **7**, 1622-1627.
28. B. L. Henke, E. M. Gullikson and J. C. Davis, *Atomic Data and Nuclear Data Tables*, 1993, **54**, 181-342.
29. H. Yuzawa, M. Nagasaka and N. Kosugi, *J. Phys. Chem. C*, 2015, **119**, 7738-7745.
30. D. Drevon, M. Görlin, P. Chernev, L. Xi, H. Dau and K. M. Lange, *Scientific Reports*, 2019, **9**, 1532.
31. A. Borgna, B. G. Anderson, A. M. Saib, H. Bluhm, M. Hävecker, A. Knop-Gericke, A. E. T. Kuiper, Y. Tamminga and J. W. Niemantsverdriet, *J. Phys. Chem. B*, 2004, **108**, 17905-17914.
32. R. Toyoshima and H. Kondoh, *J. Phys.: Condens. Matter*, 2015, **27**, 083003.
33. T. E. Jones, T. C. R. Rocha, A. Knop-Gericke, C. Stampfl, R. Schlögl and S. Piccinin, *ACS Catal.*, 2015, **5**, 5846-5850.
34. B. Eren, C. Heine, H. Bluhm, G. A. Somorjai and M. Salmeron, *J. Am. Chem. Soc.*, 2015, **137**, 11186-11190.
35. A. Knop-Gericke, M. Havecker, T. Neisius and T. Schedel-Niedrig, *Nuclear Instruments & Methods in Physics Research Section a-Accelerators Spectrometers Detectors and Associated Equipment*, 1998, **406**, 311-322.
36. M. Hävecker, A. Knop-Gericke, T. Schedel-Niedrig and R. Schlögl, *Angew. Chem., Int. Ed.*, 1998, **37**, 1939-1942.
37. A. Erbil, G. S. Cargill Iii, R. Frahm and R. F. Boehme, *Physical Review B*, 1988, **37**, 2450-2464.
38. S. L. M. Schroeder, G. D. Moggridge, R. M. Ormerod, T. Rayment and R. M. Lambert, *Surf. Sci.*, 1995, **324**, L371-L377.

39. G. Akgül, F. Aksoy, A. Bozduman, O. M. Ozkendir, Y. Ufuktepe and J. Lüning, *Thin Solid Films*, 2008, **517**, 1000-1004.
40. A. Peisert and F. Sauli, *CERN-84-08 Drift and diffusion of electrons in gases: a compilation*, 1984.
41. H. M. Rosenstock, K. Draxl, B. W. Steiner and J. T. Herron, in *NIST Chemistry WebBook, NIST Standard Reference Database Number 69*, eds. P. J. Linstrom and W. G. Mallard, National Institute of Standards and Technology, Gaithersburg MD, 2018, DOI: https://doi.org/10.18434/T4D303.
42. A. Knop-Gericke, M. Hävecker, T. Schedel-Niedrig and R. Schlögl, *Top. Catal.*, 2000, **10**, 187-198.
43. A. Knop-Gericke, M. Hävecker, T. Schedel-Niedrig and R. Schlögl, *Top. Catal.*, 2001, **15**, 27-34.
44. R. W. Mayer, M. Havecker, A. Knop-Gericke and R. Schlogl, *Catal. Lett.*, 2001, **74**, 115-119.
45. R. W. Mayer, M. Melzer, M. Hävecker, A. Knop-Gericke, J. Urban, H. J. Freund and R. Schlögl, *Catal. Lett.*, 2003, **86**, 245-260.
46. M. Abbate, J. B. Goedkoop, F. M. F. de Groot, M. Grioni, J. C. Fuggle, S. Hofmann, H. Petersen and M. Sacchi, *Surf. Interface Anal.*, 1992, **18**, 65-69.
47. A. M. J. van der Eerden, J. A. van Bokhoven, A. D. Smith and D. C. Koningsberger, *Rev. Sci. Instrum.*, 2000, **71**, 3260-3266.
48. A. Knop-Gericke, F. M. F. de Groot, J. A. van Bokhoven and T. Ressler, in *In situ spectroscopy of catlaysts*, ed. B. M. Weckhuysen, American Scientific Publishers, Portland, OR 2004, ch. 5.
49. I. J. Drake, T. C. N. Liu, M. Gilles, T. Tyliszczak, A. L. D. Kilcoyne, D. K. Shuh, R. A. Mathies and A. T. Bell, *Rev. Sci. Instrum.*, 2004, **75**, 3242-3247.
50. C. Heske, U. Groh, O. Fuchs, L. Weinhardt, E. Umbach, T. Schedel-Niedrig, C.-H. Fischer, M. C. Lux-Steiner, S. Zweigart, T. P. Niesen, F. Karg, J. D. Denlinger, B. Rude, C. Andrus and F. Powell, *The Journal of Chemical Physics*, 2003, **119**, 10467-10470.
51. J. Forsberg, L.-C. Duda, A. Olsson, T. Schmitt, J. Andersson, J. Nordgren, J. Hedberg, C. Leygraf, T. Aastrup, D. Wallinder and J.-H. Guo, *Rev. Sci. Instrum.*, 2007, **78**, 083110.
52. T. Herranz, X. Y. Deng, A. Cabot, J. G. Guo and M. Salmeron, *J. Phys. Chem. B*, 2009, **113**, 10721-10727.
53. P. Jiang, J.-L. Chen, F. Borondics, P.-A. Glans, M. W. West, C.-L. Chang, M. Salmeron and J. Guo, *Electrochem. Commun.*, 2010, **12**, 820-822.
54. A. Braun, K. Sivula, D. K. Bora, J. Zhu, L. Zhang, M. Grätzel, J. Guo and E. C. Constable, *J. Phys. Chem. C*, 2012, **116**, 16870-16875.
55. T. Ishihara, T. Tokushima, Y. Horikawa, M. Kato and I. Yagi, *Rev. Sci. Instrum.*, 2017, **88**, 104101.
56. H. Niwa, H. Kiuchi, J. Miyawaki, Y. Harada, M. Oshima, Y. Nabae and T. Aoki, *Electrochem. Commun.*, 2013, **35**, 57-60.
57. M. Hävecker, A. Knop-Gericke and T. Schedel-Niedrig, *Appl. Surf. Sci.*, 1999, **142**, 438-442.
58. W. M. Heijboer, A. A. Battiston, A. Knop-Gericke, M. Hävecker, R. Mayer, H. Bluhm, R. Schlögl, B. M. Weckhuysen, D. C. Koningsberger and F. M. F. de Groot, *J. Phys. Chem. B*, 2003, **107**, 13069-13075.
59. W. M. Heijboer, D. C. Koningsberger, B. M. Weckhuysen and F. M. F. de Groot, *Catal. Today*, 2005, **110**, 228-238.
60. M. Havecker, R. W. Mayer, A. Knop-Gericke, H. Bluhm, E. Kleimenov, A. Liskowski, D. Su, R. Follath, F. G. Requejo, D. F. Ogletree, M. Salmeron, J. A. Lopez-Sanchez, J. K. Bartley, G. J. Hutchings and R. Schlogl, *J. Phys. Chem. B*, 2003, **107**, 4587-4596.
61. F. Morales, F. M. F. de Groot, P. Glatzel, E. Kleimenov, H. Bluhm, M. Hävecker, A. Knop-Gericke and B. M. Weckhuysen, *J. Phys. Chem. B*, 2004, **108**, 16201-16207.
62. F. Zheng, S. Alayoglu, J. Guo, V. Pushkarev, Y. Li, P.-A. Glans, J.-l. Chen and G. Somorjai, *Nano Lett.*, 2011, **11**, 847-853.
63. S. Alayoglu, S. K. Beaumont, F. Zheng, V. V. Pushkarev, H. Zheng, V. Iablokov, Z. Liu, J. Guo, N. Kruse and G. A. Somorjai, *Top. Catal.*, 2011, **54**, 778-785.
64. V. Iablokov, S. K. Beaumont, S. Alayoglu, V. V. Pushkarev, C. Specht, J. H. Gao, A. P. Alivisatos, N. Kruse and G. A. Somorjai, *Nano Lett.*, 2012, **12**, 3091-3096.
65. S. K. Beaumont, S. Alayoglu, C. Specht, W. D. Michalak, V. V. Pushkarev, J. Guo, N. Kruse and G. A. Somorjai, *J. Am. Chem. Soc.*, 2014, **136**, 9898-9901.
66. F. Zheng, S. Alayoglu, V. V. Pushkarev, S. K. Beaumont, C. Specht, F. Aksoy, Z. Liu, J. Guo and G. A. Somorjai, *Catal. Today*, 2012, **182**, 54-59.
67. S. Alayoglu, S. K. Beaumont, G. Melaet, A. E. Lindeman, N. Musselwhite, C. J. Brooks, M. A. Marcus, J. G. Guo, Z. Liu, N. Kruse and G. A. Somorjai, *J. Phys. Chem. C*, 2013, **117**, 21803-21809.
68. S. Alayoglu, K. J. An, G. Melaet, S. Y. Chen, F. Bernardi, L. W. Wang, A. E. Lindeman, N. Musselwhite, J. H. Guo, Z. Liu, M. A. Marcus and G. A. Somorjai, *J. Phys. Chem. C*, 2013, **117**, 26608-26616.
69. K. An, S. Alayoglu, N. Musselwhite, S. Plamthottam, G. Melaet, A. E. Lindeman and G. A. Somorjai, *J. Am. Chem. Soc.*, 2013, **135**, 16689-16696.
70. C. Escudero, P. Jiang, E. Pach, F. Borondics, M. W. West, A. Tuxen, M. Chintapalli, S. Carenco, J. Guo and M. Salmeron, *J. Synchrotron Radiat.*, 2013, **20**, 504-508.
71. A. Tuxen, S. Carenco, M. Chintapalli, C. H. Chuang, C. Escudero, E. Pach, P. Jiang, F. Borondics, B. Beberwyck, A. P. Alivisatos, G. Thornton, W. F. Pong, J. H. Guo, R. Perez, F. Besenbacher and M. Salmeron, *J. Am. Chem. Soc.*, 2013, **135**, 2273-2278.
72. S. Carenco, A. Tuxen, M. Chintapalli, E. Pach, C. Escudero, T. D. Ewers, P. Jiang, F. Borondics, G. Thornton, A. P. Alivisatos, H. Bluhm, J. Guo and M. Salmeron, *J. Phys. Chem. C*, 2013, **117**, 6259-6266.
73. C. Castán-Guerrero, D. Krizmancic, V. Bonanni, R. Edla, A. Deluisa, F. Salvador, G. Rossi, G. Panaccione and P. Torelli, *Rev. Sci. Instrum.*, 2018, **89**, 054101.
74. P. T. Kristiansen, T. C. R. Rocha, A. Knop-Gericke, J. H. Guo and L. C. Duda, *Rev. Sci. Instrum.*, 2013, **84**, 113107.
75. T. J. Penfold, in *High-Resolution XAS/XES: Analyzing Electronic Structures of Catalysts*, ed. J. Sa, Taylor & Francis, 2014.
76. X. X. Wang, D. A. Cullen, Y.-T. Pan, S. Hwang, M. Wang, Z. Feng, J. Wang, M. H. Engelhard, H. Zhang, Y. He, Y. Shao, D. Su, K. L. More, J. S. Spendelow and G. Wu, *Adv. Mater.*, 2018, **30**, 1706758.
77. G. L. Bezemer, J. H. Bitter, H. P. C. E. Kuipers, H. Oosterbeek, J. E. Holewijn, X. Xu, F. Kapteijn, A. J. van Dillen and K. P. de Jong, *J. Am. Chem. Soc.*, 2006, **128**, 3956-3964.
78. Z.-j. Wang, S. Skiles, F. Yang, Z. Yan and D. W. Goodman, *Catal. Today*, 2012, **181**, 75-81.

79. M. E. Grass, Y. Zhang, D. R. Butcher, J. Y. Park, Y. Li, H. Bluhm, K. M. Bratlie, T. Zhang and G. A. Somorjai, *Angew. Chemie., Int. Ed.*, 2008, **47**, 8893-8896.
80. S. Sadasivan, R. M. Bellabarba and R. P. Tooze, *Nanoscale*, 2013, **5**, 11139-11146.
81. J. P. den Breejen, P. B. Radstake, G. L. Bezemer, J. H. Bitter, V. Froseth, A. Holmen and K. P. de Jong, *J. Am. Chem. Soc.*, 2009, **131**, 7197-7203.
82. Y. Miyajima, K. Yasuda and Y. Kanzawa, *Bull Tokyo Med Dent Univ*, 1976, **23**, 41-51.
83. US 6362239, 1999.
84. R. Oike, Y. Okamoto, T. Tokushima, T. Nakamura and K. Amezawa, *Electrochemistry*, 2016, **84**, 793-796.
85. P. Glatzel, T.-C. Weng, K. Kvashnina, J. Swarbrick, M. Sikora, E. Gallo, N. Smolentsev and R. A. Mori, *J. Electron Spectrosc. Relat. Phenom.*, 2013, **188**, 17-25.
86. M. Kubin, J. Kern, M. Guo, E. Källman, R. Mitzner, V. K. Yachandra, M. Lundberg, J. Yano and P. Wernet, *Phys. Chem. Chem. Phys.*, 2018, **20**, 16817-16827.